Defective cranial skeletal development, larval lethality and haploinsufficiency in Myod mutant zebrafish

Yaniv Hinits, **Victoria C. Williams**, **Dylan Sweetman**[¶], **Thomas M. Donn**[§], **Taylur P. Ma**[§], **Cecilia B. Moens**[§], and **Simon M. Hughes**[1]
Randall Division for Cell and Molecular Biophysics, New Hunt's House, Guy's Campus, King's College London, SE1 1UL, UK.

[¶]Division of Animal Sciences, School of Biosciences, University of Nottingham, Sutton Bonington Campus, Loughborough, Leics, LE12 5RD, UK.

[§]Division of Basic Science, Fred Hutchinson Cancer Center, 1100 Fairview Ave. N. PO Box 19024 Seattle, WA 98109, USA.

Summary

Myogenic regulatory factors of the *myod* family (MRFs) are transcription factors essential for mammalian skeletal myogenesis. Here we show that a mutation in the zebrafish *myod* gene delays and reduces early somitic and pectoral fin myogenesis, reduces miR-206 expression, and leads to a persistent reduction in somite size until at least the independent feeding stage. A mutation in *myog*, encoding a second MRF, has little obvious phenotype at early stages, but exacerbates the loss of somitic muscle caused by lack of Myod. Mutation of both *myod* and *myf5* ablates all skeletal muscle. Haploinsufficiency of *myod* leads to reduced embryonic somite muscle bulk. Lack of Myod causes a severe reduction in cranial musculature, ablating most muscles including the protractor pectoralis, a putative cucullaris homologue. This phenotype is accompanied by a severe dysmorphology of the cartilaginous skeleton and failure of maturation of several cranial bones, including the opercle. As *myod* expression is restricted to myogenic cells, the data show that myogenesis is essential for proper skeletogenesis in the head.

Keywords

muscle; zebrafish; myosin; slow; fiber; fast; myod; myogenin; myf5; miR-206; skeleton; bone; cartilage; head; fin; haploinsufficiency

---

Introduction

As its name implies, skeletal muscle develops and functions in intimate contact with the skeleton. It is clear that cartilage and bone can develop in the absence of skeletal muscle (Chevallier, 1979; Christ et al., 1977; Kardon, 1998). However, abundant evidence from sports science and exercise physiology shows that there is mutual dependency of muscular and skeletal maintenance and growth (Robling, 2009). Indeed, skeletal defects have been observed early in development of mice genetically modified to lack skeletal muscle. For example, mice lacking the key myogenic regulatory transcription factors (MRFs) not only lack certain early muscle fibres but also show skeletal defects (Hasty et al., 1993; Rawls et al., 1998; Rudnicki et al., 1992; Valdez et al., 2000; Venuti et al., 1995; Zhang et al., 1995).

---

[1]Corresponding author: Randall Division, 3rd floor north, New Hunt's House, Guy's Campus, King's College London, London SE1 1UL, UK. Tel.: +44 20 7848 6445; fax: +44 20 7848 6550; simon.hughes@kcl.ac.uk.

As these MRF genes are expressed only in the skeletal muscle lineage, it has been suggested that skeletal defects arise due to altered signalling between early muscle cells and skeletal precursors (Vinagre et al., 2010; Vivian et al., 2000). Additionally, alteration of expression of adjacent genes caused by the genomic manipulations may have a role, as new knockout alleles have less severe skeletal consequences (Kassar-Duchossoy et al., 2004; Kaul et al., 2000). To compare musculoskeletal developmental interactions and the roles of individual MRFs across the vertebrates, we turned to the zebrafish, in which point mutations and/or antisense morpholinos minimize genetic complications.

Like mice, zebrafish have four MRF family members: Myod, Myf5, Myogenin and Mrf4/ Myf6. Previously, we analysed *myf5* and *myf6* mutants and found rather mild defects, less pronounced at early stages than those in mice lacking these MRFs individually (Hinits et al., 2009; Kassar-Duchossoy et al., 2004; Kaul et al., 2000; Zhang et al., 1995). Mice lacking Myod also have a surprisingly mild phenotype (Rudnicki et al., 1992). In contrast, we observed severe defects in somitic and cranial myogenesis in *myod* morphant embryos (Hinits et al., 2009). These differences raise the possibility that the functions of *myf5* and *myod* have diverged during vertebrate evolution. On the other hand, the phenotype of double *myf5;myod* loss of function appears quite similar in mice and fish; most, but not all, early myogenesis is ablated (Hinits et al., 2009; Kassar-Duchossoy et al., 2004). Thus, the extent of divergence in role of MRF genes is unclear.

Here we report analysis of *myod* and *myog* mutant alleles that reveal that zebrafish Myod is essential for viability. Myod is required for most early cranial myogenesis and some early pectoral fin and somitic myogenesis. Mutants lack the ability to feed and die during the post-hatch larval period. Myotome size is reduced in *myod* mutants, prior to independent feeding. There is also a transient reduction in somite bulk in *myod* heterozygotes. Unlike mice, *myf5;myod* double mutant zebrafish lack all myogenesis at least until 5 days post fertilization (dpf). Most strikingly, the lack of cranial muscle in *myod* mutants leads to a severe deformation and failure of maturation of cranial skeletogenesis. The data indicate that early myogenesis is essential for normal head patterning.

Materials and methods

Zebrafish lines and maintenance

Wild type and transgenic lines *Tg(acta1:GFP)zf13* (Higashijima et al., 1997), *Tg(-2.2mylz2:GFP)i135* (Moore et al., 2007), *Tg(βactin:HRAS-EGFP)vu119* (Cooper et al., 2005), *myf5^{hu2022}* (Hinits et al., 2009) were maintained on King's wild type background and staging and husbandry were as described (Westerfield, 1995). *Myod^{fh261}* and m*yog^{fh265}* mutant alleles were identified by TILLING (Draper et al., 2004) and were maintained on the *AB background and genotyped by sequencing of PCR products amplified from fin clip or embryo genomic DNA using primers 5′GGACCCCAGGCTTGTTC3′ and 5′GTTGGATCTCGGACTGGA3′ for *myod,* 5′AACCGGGCCATTGTCTCCA3′ and 5′CTCCATCGGCAGGCTGTAGTAGTAGTT3′ for *myf5* and 5′TGACAGCTTTACCATCGCGCTTGA3′ and 5′GTCAGTTCACTCAACCAGCAGGAGCATGA**C**3′ for *myog* (the last contains a single base mutation for the dCAPS method, http://labs.fhcrc.org/moens/Tilling_Mutants/ index.html).

In situ mRNA hybridisation, immunohistochemistry and histology

In situ mRNA hybridisation and immunohistochemistry were performed as described (Hinits and Hughes, 2007). Fluorescein- or digoxigenin-tagged probes used were *myog* (Weinberg et al., 1996), *eng2a* (Ekker et al., 1992), *mylz2* and *myhz1* (Xu et al., 2000), *smyhc1*

(Bryson-Richardson et al., 2005), actin (*acta1b,* IMAGE 7284336), *dlx2a* (Akimenko et al., 1994), *klf2b* (Oates et al., 2001). Dual-digoxigenin-labelled miR-206 specific LNA probes were obtained from Exiqon and hybridised and washed at 50 °C as described in (Sweetman et al., 2008). Antibodies were against Myod and Pax3/7 (Hammond et al., 2007), Myog (Hinits et al., 2009), striated muscle myosin heavy chain (MyHC; A4.1025 (Blagden et al., 1997) or MF20 (DHSB)), slow MyHC (F59; Devoto et al., 1996) and Smooth muscle Myosin (Myh11, Biomedical Technologies). Stains with alcian blue for cartilage and alizarin red for ossified bone was as described (Walker and Kimmel, 2007), followed by dissection to separate upper and lower head skeleton. 4,5-Diaminofluorescein diacetate (DAF-2DA, Santa Cruz) staining of bone was as described (Grimes et al., 2006).

Embryo manipulation

Myod MO (Gene-Tools, 5′-ATATCCGACAACTCCATCTTTTTTG-3′) was injected into 1-2 cell stage embryos at 4 ng/embryo. Cyclopamine (100 μM in fish medium) or vehicle control was added at 50% epiboly to embryos whose chorions had been punctured with a 30 G hypodermic needle.

Muscle size analysis

Tg(βactin:HRAS-EGFP)vu119 fish were bred onto *myod^{fh261}* and live 0.2 mM 1-phenyl-2-thiourea-treated embryos hemizygous for ßactin:GFP were embedded in 1.5% low melting point agarose in fish water containing MS222, and imaged by confocal microscopy on a Zeiss Exciter using a 20x1.0 W dipping objective on successive days. Fish were released from the agarose each day. A single lateral image and three equi-spaced transverse images within somite 17 were collected from each embryo at each stage. The somite was outlined in Zen software and an average transverse area calculated. This area was multiplied by the somite length, measured at the horizontal myoseptum, to yield an estimate of somite volume for each fish at each stage. After analysis, individual embryos were genotyped by sequencing of genomic PCR. Data are presented as mean ± s.e.m. with the number of embryos at each developmental stage indicated. Somite volume of fixed MF20-stained 72 hpf embryos was calculated similarly, and genotyped as mutants or sibs according to head muscle immunostaining. Data was analysed by two way ANOVA showing significant effect of both age and genotype using Graphpad Prism 4.0. Adult (15 month) fish from a single tank were anaesthetised, weighed and length measured, then tail-clipped for genotyping by sequencing of genomic PCR.

Results

Myod mutation delays slow and reduces fast myogenesis

TILLING (Draper et al., 2004) was used to isolate a zebrafish mutant in *myod* with a stop codon at residue 126 early in the second helix, thereby generating a predicted null mutation (Fig. 1A; (Davis et al., 1990; Ma et al., 1994)). One quarter of embryos from a carrier in-cross of *myod$^{fh261/+}$* lacked Myod immunoreactivity. DNA sequencing of individual stained embryos confirmed that those lacking Myod were mutants and that heterozygotes had less staining than wild types (Fig. 1B; quantification of all experiments is presented in Table S1). *Myod* mRNA was reduced in heterozygotes and greatly diminished in mutants at 10 somite stage (10s), suggesting nonsense-mediated decay of the mutant mRNA (Fig. 1C). Consistent with the result of morpholino (MO) knockdown of Myod, slow myogenesis was delayed in mutants (Fig. 1B)(Hinits et al., 2009). In adaxial precursors of superficial slow fibres, *myog* mRNA and other muscle differentiation markers examined were expressed, although delayed (Fig. 1D). However, *eng2a*, a marker of the specialised muscle pioneer cells, was diminished (Fig. 1E). Thus, this mutant confirms that Myod contributes to, but is not essential for, early slow myogenesis (Hinits et al., 2009).

Loss of Myod caused more dramatic defects in fast myogenesis in the somite. Early *myog* and later *mylz2* and *myhz1* myosin mRNAs were diminished in fast muscle (Fig. 1D,F). Conversely, Pax3/7, a marker of dermomyotome was up-regulated in the lateral somite at 24 hpf, with more Pax3/7-immunoreactive nuclei in sections of mutants (Fig. 1F). In summary, fast myogenesis was reduced in *myod*^*fh261*^ mutants, extending results from MO knockdown studies (Hammond et al., 2007; Hinits et al., 2009; Maves et al., 2007).

Myogenin cooperates with Myod in fast myogenesis

Myogenin is a Myod target gene. We previously suggested that Myogenin cooperates with Myod in somitic fast myogenesis (Hinits et al., 2009). We isolated a *myog*^*fh265*^ mutant by TILLING, which has a stop codon in place of residue 167, just downstream of the helix-loop-helix domain (Fig. 2A). As with *myod*, *myog* mRNA was reduced in heterozygotes and greatly diminished in mutants at 10s, suggesting nonsense-mediated decay of the mutant mRNA (Fig. 2B). Although Myog immunoreactivity was lost in mutants, no defect was observed either in in-crosses from heterozygous *myog*^*fh265/+*^ carrier fish or in genotyped *myog*^*fh265/+*^ mutants: pectoral fin, jaw and somite morphology and movement appeared normal, at least until 5 dpf (Fig. 2C,D and data not shown). However, to date no *myog*^*fh265/+*^ mutants were obtained among in-cross progeny genotyped at 10 weeks of age.

To test the hypothesis that Myod and Myog cooperate to drive fast myogenesis, *myod* MO was injected into a *myog*^*fh265/+*^ in-cross. In siblings, *myod* MO alone reduced *myhz1* expression to a similar extent to that observed in *myod*^*fh261*^ mutants (Fig. 2E, compare to Fig. 1F). In 25% of embryos from a *myog*^*fh265/+*^ incross, *myod* MO elicited an exacerbated loss of fast *myhz1* mRNA (Fig. 2E). We conclude that although full length Myog is dispensable for embryonic development, it functions to promote early fast myogenesis in the somite in co-operation with Myod.

Myod promotes miR-206 expression

Myod drives normal fast muscle differentiation in zebrafish acting, in part, through induction *myog* (Hinits et al., 2009). By 72 hpf, *myog* mRNA has declined in differentiated muscle, although its expression in dorsal and ventral somite extremes is still Myod-dependent, suggesting that Myod is required for ongoing myogenesis (Fig. 3D). miR-206 is a muscle-specific microRNA that, like Myog, has been suggested to promote myoblast differentiation (Hirai et al., 2010). In zebrafish, miR-206 expression was similar to that of *myog* in early stage somites, accumulating weakly in adaxial slow fibres as they terminally differentiate, and more strongly in medial fast muscle as it formed (Figs 1D, S1A). At 24 hpf, miR-206 was abundant in fast muscle of the somite (Fig. S1) and at later stages also in head and pectoral fin muscle, persisting beyond *myog* in differentiated fast fibres (Fig. S1B-D). Ablation of Myod function, either in *myod*^*fh261*^ or morphants, led to down-regulation of miR-206 in both slow and fast cells at 15s, although faint signal in the PSM was unchanged (Fig. 1D). Lateral miR-206 is also reduced by lack of Hh signalling, suggesting that either expression persists in slow fibres at 24 hpf or Hh signalling is required for miR-206 expression in some fast muscle (Fig. S1E). At this stage, miR-206 is clearly reduced in fast muscle of the *myod*^*fh261*^ mutant (Fig. S1E). Reduction in miR-206 persisted during the pre-hatching period after loss of *myod* function (Fig. 3A,B), and was comparable in *myod* morphants and *myod*^*fh261*^ mutant (Fig. 3C,D). By contrast, no alteration in miR-206 was detected at 15s, 24 or 48 hpf embryos from a *myf5*^*hu2022/+*^ in-cross (data not shown). These findings suggest that miR-206 accumulates in differentiating muscle fibres and that its loss could contribute to the reduction in muscle differentiation observed at 24 hpf in *myod*^*fh261*^ mutants.

The reduction in miR-206 accumulation appeared to be greater than the loss of overall muscle mass in $myod^{fh261}$ mutants at 48 hpf (Fig. 3B). Congruently, $myod^{fh261/+}$ heterozygotes showed a reduction in miR-206 compared to wild types (Fig. 3A). These data suggest that Myod function up-regulates miR-206 in differentiated muscle fibres.

Myod requirement for somitic myogenesis appears transient

The reduction in miR-206 suggested that muscle growth might be decreased in $myod^{fh261}$ mutants. *Myod* morphants have reduced muscle differentiation at 24 hpf, but growth did occur between 24 and 72 hpf ((Hinits et al., 2009); Fig. 3C). We used the $myod^{fh261}$ mutant to test whether this growth was truly Myod-independent or reflected loss of MO effectiveness. At 24 hpf, $myod^{fh261}$ mutants had approximately half the somite volume of wild type siblings. Strikingly, even heterozygous $myod^{fh261/+}$ embryos had significantly reduced somite volume, intermediate between wild type and mutant siblings (Fig. 3E). These differences appear to be maintained at 48 hpf (Fig. 3A). At 72 hpf, both *myhz1*- and miR-206-expressing tissue was reduced, as in *myod* morphants (Fig. 3C,D). In parallel, $myod^{fh261}$ mutants had reduced myotome volume compared to siblings (Fig. 3E). Significant somite growth was, nevertheless, observed in $myod^{fh261}$ mutants between 24, 72 and 120 hpf (Fig. 3A-E; P<0.001). At 120 hpf, $myod^{fh261}$ mutants were slightly smaller than wild type siblings, but increase in somite volume since 24 hpf seemed to have been normal (Fig. 3E). Studies of growth after 5 dpf were not possible in mutants owing to cranial defects (see below). We conclude that Myod is required for normal somitic myogenesis and its lack leads initially to smaller muscle bulk.

At 24 hpf, heterozygotes had significantly less somitic muscle than wild type siblings, but this defect became less significant in larvae (Fig. 3E). We compared the growth into adulthood of fish with one or two functional copies of the *myod* gene. Heterozygous $myod^{fh261/+}$ fish survived well to adulthood, and were not significantly lighter than their wild type siblings (P = 0.27; Fig 3F). Fish growth is difficult to measure because any slight size advantage leads to success in competition for food and consequent faster growth. We used fish length to control for overall growth differences. Heterozygotes were not significantly different in length from wild type (P = 0.36; Fig. 3F). These data show that loss of one *myod* allele has little effect on growth of zebrafish.

Myod drives cranial and pectoral fin myogenesis

Like *myod* morphants, $myod^{fh261}$ mutants lacked miR-206 in most cranial muscle at 72 hpf, with the exception of the sternohyoideus muscle (Fig. 4A). Other cranial muscle markers, *myog*, *myhz1* and myosin accumulation, were also greatly reduced or entirely absent (Fig. 4B-D). Fin muscle was also diminished (Fig. 4B-E), but to a variable extent amongst mutant embryos, with 68% showing bilaterally symmetrical reduction (28/41) and 32% (13/41) having asymmetry between fins of the same embryo, with greater reduction on the right more common (11/13 P = 0.013 X^2; Fig. 4E). Similarly, the levator and adductor operculi muscles were often present but reduced in fibre number. In contrast, the adjacent dilatator operculi and adductor hyomandibulae and most other cranial muscles were missing (Fig. 4F). These data confirm our morphant finding that Myod is the primary MRF driving early myogenesis in cranial and pectoral fin muscles (Hinits et al., 2009).

We examined the effect of loss of Myod on various other muscles linking the hypobranchial and pectoral regions. Whereas sternohyoideus was substantially preserved, most other muscles were reduced or missing entirely in $myod^{fh261}$ mutants. However, small groups of *myhz1*-expressing cells are observed in the pectoral zone (Fig. 4C,E). We analysed the protractor pectoralis, in particular, because this is thought to be the teleost homologue of the cucullaris muscle group (Diogo et al., 2008; Greenwood and Lauder, 1981). Looking

anterior to the cleithrum, no protractor pectoralis or levator 5 muscles were detected in *myod*^{fh261} mutants (Fig. 4F).

Lack of Myod is larval lethal. At embryonic stages, *myod*^{fh261} mutants were identified by sequence genotyping at the expected frequencies. In breeding programmes, we have not found an homozygous mutant at 13 dpf or beyond. We also separated *myod*^{fh261} mutant embryos from siblings at 5 dpf, when cranial defects become apparent (Fig. 5A) and reared them with feeding. Whereas all siblings survived (36/36), all *myod*^{fh261} mutant embryos died (9/9) in the period 6-12 dpf, presumably due to failure to feed.

Myod is essential for normal cranial skeletogenesis

By 5 dpf, *myod*^{fh261} mutants lacking cranial muscle have a striking morphological defect of the mouth (Fig. 5A). The defect was phenocopied in *myod* morphants, eliminating the possibility that a second mutation linked to the *myod*^{fh261} allele accounts for the skeletal defects (Fig. 5A). At 5 dpf, Meckel's and ceratohyal cartilages are down-turned, giving a permanently open protruding mouth (Fig. 5B). Dissection and flatmounting of cranial cartilages revealed that all major cartilage elements are present at 6 dpf (Fig. 5C). However, the morphology of chondrocytes in the head of the palatoquadrate was rounded in *myod*^{fh261} mutants and they failed to form the stacks observed in siblings, correlating with failure of morphogenesis of the joint articulation between Meckel's and palatoquadrate cartilages (Fig. 5C). We conclude that Myod function is required for aspects of cranial cartilage morphogenesis.

Some dermal bones, such as the opercle, cleithrum, and parasphenoid, which form directly from mesenchyme, were reduced or missing at 5 dpf in *myod*^{fh261} mutants (Fig. 5B). A day later, ossified cleithrum and parasphenoid were apparent, but the opercle was still missing. Moreover, ossification of cartilaginous bones such as the ceratobranchial 5 was reduced (Fig. 5C). Myod is therefore required for normal formation of bone.

No skeletal defects were observed in *myod*^{fh261} mutants prior to, or at, the normal time of cranial muscle differentiation at 3 dpf (Fig. 6A-C). We examined *dlx2a* mRNA, which is a transcription factor expressed in branchial arch skeletal precursors, *klf2b* mRNA, another transcription factor which prefigures cartilage formation, and the fluorescent nitric oxide indicator 4,5-diaminofluorescein diacetate (DAF-2DA), which strongly labels dermal bones (Lepiller et al., 2007). None was disrupted in *myod*^{fh261} mutants at 72 hpf (Fig. 6A-C). Thus, the striking skeletal defects in *myod*^{fh261} mutants only arise after the failure of muscle formation, consistent with the restriction of *myod* mRNA to myogenic zones.

Myf5 and Myod are essential for embryonic myogenesis

Myf5 and *myod* double morphants lack muscle at 15s (Hammond et al., 2007; Maves et al., 2007), but by 24 hpf small amounts of somitic muscle form even in *myf5*^{hu2022} mutants treated with *myod* morpholino (Hinits et al., 2009). To test whether this muscle is formed independent of both Myf5 and Myod activities, we bred double mutant *myf5*^{hu2022};*myod*^{fh261} fish. Such embryos lacked all muscle differentiation at 15s (Fig. S2A). Even a single functional *myf5* allele was sufficient for partial differentiation at this stage. At 24 hpf, neither slow nor fast muscle was found in the double mutants (Fig. 7A,B and Fig. S2B), suggesting that the residual muscle we observed in *myf5*^{hu2022}mutant+*myod* MO (see (Hinits et al., 2009)) differentiated due to inefficiency of the *myod* MO. All cranial, pectoral fin and somitic muscle was entirely lacking at 72 and 120 hpf (Fig. 7C,D and Fig. S2C-E), indicating that either Myf5 or Myod is essential for early myogenesis in the zebrafish.

Double mutant *myf5^hu2022^*;*myod^fh261^* fish show cranial skeletal defects more severe than those of *myod^fh261^* single mutants (Fig. 7E). As both *myod^fh261^* and *myf5^hu2022^*;*myod^fh261^* mutant fish die prior to trunk skeletogenesis, the effect of muscle loss on vertebral and rib development could not be assessed. However, the skeletons of adult *myod^fh261/+^* and 13 dpf *myod^fh261/+^* and *myf5^hu2022/+^*;*myod^fh261/+^* dual heterozygous fish showed no consistent defects (data not shown). Among the cohort of fish analysed at 13 dpf no *myf5^hu2022^*;*myod^fh261/+^* or *myf5^hu2022^* mutants were found among 30 larvae analysed, showing that these genotypes fail to survive.

Discussion

The findings described here provide genetic demonstration of three major points. First, that Myod is essential for viability, normal somite and limb myogenesis and most of cranial myogenesis in zebrafish. Second, that either *myf5* or *myod* is essential for all embryonic muscle differentiation. Third, that formation of a normal cranial skeleton is dependent upon the proper generation of musculature.

MRF roles in muscle development

We previously suggested, based on morpholino knockdown experiments, that *myod* functions to drive differentiation of a specific subset of somitic muscle fibres (Hinits et al., 2009). The results presented here provide independent genetic confirmation that Myod is essential for both cranial and somitic myogenesis. We show here that, in zebrafish, Myod is essential for viability, in sharp contrast to mice in which *Myod1* null mutants are viable and fertile (Rudnicki et al., 1992). The molecular nature of *myod^fh261^* and the severity of the phenotype suggest that the allele is a functional null. As a truncated N-terminal peptide could theoretically be produced in *myod^fh261^*, either the truncated protein is not significantly accumulated or the in vitro finding that a Myod protein lacking the second helix loses its ability to bind DNA, dimerise and function in myogenesis (Davis et al., 1990)) is also true for Myod function in vivo. In this regard, we note that the mutant *myod* mRNA is less abundant, probably due to nonsense-mediated decay, indicating a low translation rate of the truncated N-terminal peptide.

We describe a persistent somitic muscle defect in *myod^fh261^* mutants, at least until 5 dpf, when lack of ability to feed complicates further analysis (see below). Nevertheless, significant somitic muscle growth does occur during the larval period. Myf5 is required for this growth, as *myf5*;*myod* double mutants fail to make any skeletal muscle. The *myf5*-dependent cells do not fully compensate for lack of Myod. Yet Myf5 can support significant pre-hatching growth in *myod^fh261^* mutants, despite the low levels of *myf5* mRNA detected at these stages. Numerous minor defects are present in *Myod* mutant mice, even though they are viable (Brack et al., 2005; Chargé et al., 2008; Hughes et al., 1997; Megeney et al., 1996; Tiidus et al., 1996; Wang et al., 2003; Yablonka-Reuveni et al., 1999). *MyoD^m1^* mutant mice show poor postnatal survival when in competition with littermates carrying a wild type *MyoD* allele, but survive well without such competition (Rudnicki et al., 1992). In the case of *myod^fh261^* mutant zebrafish, by contrast, all mutants fail to survive in bulk rearing, in which competition for resources is less intense than in mouse pups, and even when reared alone. It seems that despite elements of redundancy between Myf5 and Myod, a significant role for each explains their conservation across the vertebrates.

The identification of haploinsufficiency in *myod^fh261/+^* embryos demanded detailed study. By comparing fish of molecularly verified genotype, we describe both a significant reduction in Myod protein immunoreactivity and miR-206 at early stages and a reduction of embryonic muscle bulk in *myod^fh261/+^* heterozygotes. Haploinsufficiency in MyoD and Mrf4 has been observed at the molecular level in mice (Patapoutian et al., 1995; Rudnicki et

al., 1992). In humans, haploinsufficiency in Mrf4 has been suggested to exacerbate muscular dystrophy (Kerst et al., 2000). With growth during the larval period, the muscle defect in $myod^{fh261/+}$ heterozygotes appears to diminish, at least as a proportion of total muscle bulk. Adult $myod^{fh261/+}$ heterozygous fish had no significant growth defect.

Pectoral fin muscle derives from cells of somitic origin (Neyt et al., 2000). Fin muscle was delayed and diminished in $myod^{fh261}$ mutants, although some fin movement was observed by 5 dpf. This confirms our finding of variable defects in fin musculature in $myod$ morphants and is consistent with the delayed limb myogenesis in $MyoD1$ mutant mice (Chen and Goldhamer, 2004; Hinits et al., 2009; Kablar et al., 1997). Recent analyses have highlighted the importance in amniotes and basal chordates of the cucullaris muscle group that links forelimb and neck movement and stabilizes the shoulder girdle (Kusakabe et al., 2011; Theis et al., 2011). The development and even the existence of cucullaris muscles in teleosts has been unclear, as the group is reduced and appears to develop late, being known as the protractor pectoralis (Diogo et al., 2008; Greenwood and Lauder, 1981). The zebrafish protractor pectoralis depends on Myod for its formation, like many other head muscles. However, as some somitic myogenesis is also Myod-dependent, our finding does not address the developmental origin of the teleost protractor pectoralis.

Although most intrinsic head muscle are consistently missing in $myod^{fh261}$ mutants, remnants of certain head muscles are observed. Variable loss of each individual branchiomeric muscle occurs in $Tbx1$ mutant mice and only posterior arch muscles are lost in $tbx1$ mutant zebrafish (Kelly et al., 2004; Piotrowski and Nusslein-Volhard, 2000). In contrast, we observe a consistent loss of some muscles in all arches, and a size reduction of other muscles in the first two arches. Vestiges of both the adductor mandibulae, the putative masseter homologue, and two specific hyoid arch muscles, adductor operculi and levator operculi are identifiable based on their location and orientation in $myod^{fh261}$ mutants. Both adductor muscles appear to be common osteichthyan plesiomorphies (Diogo et al., 2008). The greater role of Myf5 in these muscles is reminiscent of the situation in mice, in which either Myf5 or MyoD is sufficient for head myogenesis (reviewed in (Sambasivan et al., 2011). Most strikingly, it is precisely the two hyoid opercular muscles that remain in $myod^{fh261}$ mutants that are partially lost in Ret signalling mutants, raising the possibility of complementary mechanisms of myogenesis (Knight et al., 2011).

The $myog^{fh265}$ mutant had little phenotype in both somitic and cranial muscles, and was thus much milder than we previously reported in $myog$ morphants (Hinits et al., 2009). However, on a $myod^{fh261}$ mutant background, $myog^{fh265}$ caused a loss of fast muscle similar to, but less extensive than, that caused by $myog$ MO. These findings raise the possibility that the $myog^{fh265}$ allele is hypomorphic. Using an antiserum raised to the entire Myogenin protein, but for which the major epitopes are unknown, we could not detect protein in $myog^{fh265}$ mutants. Nevertheless, an in vitro study in which the introduction of a termination codon $3'$ of the HLH motif of mouse Myogenin (a similar change to the $myog^{fh265}$ allele) resulted in a partial, rather than a complete, loss in myogenic activity (Schwarz et al., 1992). Clarification of the role of Myog in fish awaits isolation of an unambiguous null allele.

The lack of skeletal muscle in $myf5;myod$ double mutants shows that zebrafish Mrf4 alone cannot drive early somitic myogenesis, unlike the situation in the mouse (Kassar-Duchossoy et al., 2004). Our data raise the possibility that, early in vertebrate evolution, Myf5 and Myod were the primary MRF drivers of myogenesis and that Mrf4 secondarily gained a myogenic role, somewhere in the amniote lineage. Alternatively, zebrafish could have lost an early role for Mrf4 present in the common ancestor. In either case, our data predict that, although $Mrf4$ and $Myf5$ have retained close genetic linkage for at least 400 Myr, the

regulation in the locus has diverged significantly. Mrf4 clearly evolved prior to the divergence of sarcopterygian and actinopterygian fish (Atchley et al., 1994). The major conserved site of expression of *Mrf4* is in differentiated muscle fibres, so it is likely that its ancestral role was in these cells and that elements controlling fibre expression may be conserved across the vertebrates (Hinits et al., 2007).

Myod regulation of miR-206 in vivo

miR-206 is expressed primarily in zebrafish differentiated muscle of both slow and fast lineages in somitic, limb and cranial muscles. Like mice, zebrafish lacking Myod express miR-206 in their muscle (Sweetman et al., 2008). The loss of miR-206 in $myod^{fh261}$ mutant cranial regions is most simply explained by the loss of cranial muscles in the $myod^{fh261}$ mutant. However, the loss of miR-206 in the trunk musculature is less readily explained by loss of muscle cells, because miR-206 appears more highly reduced than *myhz1* mRNA. In contrast, the apparently normal accumulation of miR-206 in $myf5^{hu2022}$ mutant fish, is quite different from the lack of miR-206 in somitic muscle of *Myf5* mutant mice until at least E14, when muscle is already differentiated (Sweetman et al., 2008). miR-206 can drive muscle differentiation and promote cell survival in mammals by regulating Pax3/7 genes (Dey et al., 2011; Hirai et al., 2010; Rao et al., 2006). Lack of miR-206 accumulation may contribute to the maintenance of Pax3/7 in extra cells we observe in the somite of $myod^{fh261}$ mutant fish. However, based on its abundant expression, the major function of miR-206 in fish appears to be in muscle fibres themselves, consistent with its reported role in neuromuscular interaction (Williams et al., 2009).

Effect of muscle development on skeletogenesis

The data presented show that Myod, and presumably muscle, are essential for proper development of the ventral head, jaw and pectoral girdle. Not only muscle, but also skeletal and, presumably, connective tissue elements are affected. These cranial defects prevent survival of *myod* mutant fish beyond larval development. This finding is phenocopied in *myod* morphants. Therefore, effects on adjacent genes or other genetic changes arising during the tilling screen can be eliminated as contributing to the phenotype.

Myod mutant mice show no defects in skeletogenesis, presumably reflecting the ability of Myf5 to compensate for loss of Myod in mouse cranial myogenesis (Sambasivan et al., 2009). However, mice with no muscles or with reduced muscle mass, such as mutants affecting the *Mrf4/Myf5* locus, *Myf5;Myod* double mutants and *Pax3* (Splotch) mutants have dramatic skeletal defects, the origin of which is complex (Gensch et al., 2008; Haldar et al., 2008; Kassar-Duchossoy et al., 2004; Kaul et al., 2000; Nowlan et al., 2010; Vinagre et al., 2010). Unlike *myf5*, *myod* lacks synteny between fish and mammals (www.metazome.org) and, more importantly, is not significantly expressed in presomitic mesoderm. So a cell autonomous function of Myod in skeletogenic cells is unlikely, as suggested in mice (Vinagre et al., 2010). We conclude that lack of myogenesis per se leads to skeletal defects.

The head phenotype of $myod^{fh261}$ mutant fish bears some similarity to the open mouth and cranial cartilage defects resulting from mutation of *mef2ca (hoover)* (Miller et al., 2007). Elegant transplantation experiments in fish and lineage-specific deletion of *Mef2c* in mouse have shown a cell autonomous requirement for Mef2ca in neural crest-derived cartilage cells (Miller et al., 2007; Verzi et al., 2007). *Mef2ca* is expressed in both cranial neural crest and muscle (Hinits and Hughes, 2007; Miller et al., 2007). In contrast, *myod* expression is only detected in myogenic cells (Hinits et al., 2009; Weinberg et al., 1996), showing that it acts on cartilage and bone non-cell autonomously. As *mef2ca* is expressed in muscle cells after

terminal differentiation (Hinits and Hughes, 2007), our data raise the possibility that defects in muscle fibre function may also contribute to the *mef2ca* mutant skeletal phenotype.

The effects of the lack of head muscle differentiation on the cranial bone and cartilage elements, make the zebrafish *myod* mutant an excellent model to study the signalling events and interactions between these tissues.

Supplementary Material

Refer to Web version on PubMed Central for supplementary material.

Acknowledgments

References

Akimenko MA, Ekker M, Wegner J, Lin W, Westerfield M. Combinatorial expression of three zebrafish genes related to distal-less: part of a homeobox gene code for the head. J. Neurosci. 1994; 14:3475–3486. [PubMed: 7911517]

Atchley WR, Fitch WM, Bronner-Fraser M. Molecular evolution of the MyoD family of transcription factors. Proc. Natl Acad. Sci. USA. 1994; 91:11522–11526. [PubMed: 7972095]

Blagden CS, Currie PD, Ingham PW, Hughes SM. Notochord induction of zebrafish slow muscle mediated by Sonic Hedgehog. Genes Dev. 1997; 11:2163–2175. [PubMed: 9303533]

Brack AS, Bildsoe H, Hughes SM. Evidence that satellite cell decrement contributes to preferential decline in nuclear number from large fibres during murine age-related muscle atrophy. J Cell Sci. 2005; 118:4813–4821. [PubMed: 16219688]

Bryson-Richardson RJ, Daggett DF, Cortes F, Neyt C, Keenan DG, Currie PD. Myosin heavy chain expression in zebrafish and slow muscle composition. Dev. Dyn. 2005; 233:1018–1022. [PubMed: 15830374]

Chargé SB, Brack AS, Bayol SA, Hughes SM. MyoD- and nerve-dependent maintenance of MyoD expression in mature muscle fibres acts through the DRR/PRR element. BMC Dev. Biol. 2008; 8:5. [PubMed: 18215268]

Chen JC, Goldhamer DJ. The core enhancer is essential for proper timing of MyoD activation in limb buds and branchial arches. Dev. Biol. 2004; 265:502–512. [PubMed: 14732408]

Chevallier A. Role of the somitic mesoderm in the development of the thorax in bird embryos. II. Origin of thoracic and appendicular musculature. J. Embryol. Exp. Morphol. 1979; 49:73–88. [PubMed: 448278]

Christ B, Jacob HJ, Jacob M. Experimental analysis of the origin of the wing musculature in avian embryos. Anat. Embryol. (Berl). 1977; 150:171–186. [PubMed: 857700]

Cooper MS, Szeto DP, Sommers-Herivel G, Topczewski J, Solnica-Krezel L, Kang HC, Johnson I, Kimelman D. Visualizing morphogenesis in transgenic zebrafish embryos using BODIPY TR methyl ester dye as a vital counterstain for GFP. Dev. Dyn. 2005; 232:359–368. [PubMed: 15614774]

Davis RL, Cheng PF, Lassar AB, Weintraub H. The MyoD DNA binding domain contains a recognition code for muscle-specific gene activation. Cell. 1990; 60:733–746. [PubMed: 2155707]

Devoto SH, Melancon E, Eisen JS, Westerfield M. Identification of separate slow and fast muscle precursor cells in vivo, prior to somite formation. Development. 1996; 122:3371–3380. [PubMed: 8951054]

Dey BK, Gagan J, Dutta A. miR-206 and -486 induce myoblast differentiation by downregulating Pax7. Mol. Cell. Biol. 2011; 31:203–214. [PubMed: 21041476]

Diogo R, Hinits Y, Hughes SM. Development of mandibular, hyoid and hypobranchial muscles in the zebrafish: homologies and evolution of these muscles within bony fishes and tetrapods. BMC Dev. Biol. 2008; 8:24. [PubMed: 18307809]

Draper BW, McCallum CM, Stout JL, Slade AJ, Moens CB. A high-throughput method for identifying N-ethyl-N-nitrosourea (ENU)-induced point mutations in zebrafish. Methods Cell Biol. 2004; 77:91–112. [PubMed: 15602907]

Ekker M, Wegner J, Akimenko MA, Westerfield M. Coordinate embryonic expression of three zebrafish *engrailed* genes. Development. 1992; 116:1001–1010. [PubMed: 1363539]

Gensch N, Borchardt T, Schneider A, Riethmacher D, Braun T. Different autonomous myogenic cell populations revealed by ablation of Myf5-expressing cells during mouse embryogenesis. Development. 2008; 135:1597–1604. [PubMed: 18367555]

Greenwood PH, Lauder GV. The protractor pectoralis muscle and the classification of teleost fishes. Bulletin of the British Museum (Natural History). Zoology. 1981; 41:213–234.

Grimes AC, Stadt HA, Shepherd IT, Kirby ML. Solving an enigma: arterial pole development in the zebrafish heart. Dev. Biol. 2006; 290:265–276. [PubMed: 16405941]

Haldar M, Karan G, Tvrdik P, Capecchi MR. Two Cell Lineages, myf5-Dependent and myf5-Independent, Participate in Mouse Skeletal Myogenesis. Dev. Cell. 2008; 14:437–445. [PubMed: 18331721]

Hammond CL, Hinits Y, Osborn DP, Minchin JE, Tettamanti G, Hughes SM. Signals and myogenic regulatory factors restrict pax3 and pax7 expression to dermomyotome-like tissue in zebrafish. Dev. Biol. 2007; 302:504–521. [PubMed: 17094960]

Hasty P, Bradley A, Morris JH, Edmondson DG, Venuti JM, Olson EN, Klein WH. Muscle deficiency and neonatal death in mice with targeted mutation in the *myogenin* gene. Nature. 1993; 364:501–506. [PubMed: 8393145]

Higashijima S, Nose A, Eguchi G, Hotta Y, Okamoto H. Mindin/F-spondin family: novel ECM proteins expressed in the zebrafish embryonic axis. Dev. Biol. 1997; 192:211–227. [PubMed: 9441663]

Hinits Y, Hughes SM. Mef2s are required for thick filament formation in nascent muscle fibres. Development. 2007; 134:2511–2519. [PubMed: 17537787]

Hinits Y, Osborn DP, Carvajal JJ, Rigby PW, Hughes SM. Mrf4 (myf6) is dynamically expressed in differentiated zebrafish skeletal muscle. Gene Expr. Patterns. 2007; 7:738–745. [PubMed: 17638597]

Hinits Y, Osborn DP, Hughes SM. Differential requirements for myogenic regulatory factors distinguish medial and lateral somitic, cranial and fin muscle fibre populations. Development. 2009; 136:403–414. [PubMed: 19141670]

Hirai H, Verma M, Watanabe S, Tastad C, Asakura Y, Asakura A. MyoD regulates apoptosis of myoblasts through microRNA-mediated down-regulation of Pax3. J. Cell Biol. 2010; 191:347–365. [PubMed: 20956382]

Hughes SM, Koishi K, Rudnicki M, Maggs AM. MyoD protein is differentially accumulated in fast and slow skeletal muscle fibres and required for normal fibre type balance in rodents. Mech. Dev. 1997; 61:151–163. [PubMed: 9076685]

Kablar B, Krastel K, Ying C, Asakura A, Tapscott SJ, Rudnicki MA. MyoD and Myf-5 differentially regulate the development of limb versus trunk skeletal muscle. Development. 1997; 124:4729–4738. [PubMed: 9428409]

Kardon G. Muscle and tendon morphogenesis in the avian hind limb. Development. 1998; 125:4019–4032. [PubMed: 9735363]

Kassar-Duchossoy L, Gayraud-Morel B, Gomes D, Rocancourt D, Buckingham M, Shinin V, Tajbakhsh S. Mrf4 determines skeletal muscle identity in Myf5:Myod double-mutant mice. Nature. 2004; 431:466–471. [PubMed: 15386014]

Kaul A, Koster M, Neuhaus H, Braun T. Myf-5 revisited: loss of early myotome formation does not lead to a rib phenotype in homozygous Myf-5 mutant mice. Cell. 2000; 102:17–19. [PubMed: 10929709]

Kelly RG, Jerome-Majewska LA, Papaioannou VE. The del22q11.2 candidate gene Tbx1 regulates branchiomeric myogenesis. Hum. Mol. Genet. 2004; 13:2829–2840. [PubMed: 15385444]

Kerst B, Mennerich D, Schuelke M, Stoltenburg-Didinger G, von Moers A, Gossrau R, van Landeghem FK, Speer A, Braun T, Hubner C. Heterozygous myogenic factor 6 mutation associated with myopathy and severe course of Becker muscular dystrophy. Neuromuscul. Disord. 2000; 10:572–577. [PubMed: 11053684]

Knight RD, Mebus K, d'Angelo A, Yokoya K, Heanue T, Roehl H. Ret signalling integrates a craniofacial muscle module during development. Development. 2011; 138:2015–2024. [PubMed: 21490065]

Kusakabe R, Kuraku S, Kuratani S. Expression and interaction of muscle-related genes in the lamprey imply the evolutionary scenario for vertebrate skeletal muscle, in association with the acquisition of the neck and fins. Dev. Biol. 2011; 350:217–227. [PubMed: 21035440]

Lepiller S, Laurens V, Bouchot A, Herbomel P, Solary E, Chluba J. Imaging of nitric oxide in a living vertebrate using a diamino-fluorescein probe. Free Radic. Biol. Med. 2007; 43:619–627. [PubMed: 17640572]

Ma PC, Rould MA, Weintraub H, Pabo CO. Crystal structure of MyoD bHLH domain-DNA complex: perspectives on DNA recognition and implications for transcriptional activation. Cell. 1994; 77:451–459. [PubMed: 8181063]

Maves L, Waskiewicz AJ, Paul B, Cao Y, Tyler A, Moens CB, Tapscott SJ. Pbx homeodomain proteins direct Myod activity to promote fast-muscle differentiation. Development. 2007; 134:3371–3382. [PubMed: 17699609]

Megeney LA, Kablar B, Garrett K, Anderson JE, Rudnicki MA. MyoD is required for myogenic stem cell function in adult skeletal muscle. Genes Dev. 1996; 10:1173–1183. [PubMed: 8675005]

Miller CT, Swartz ME, Khuu PA, Walker MB, Eberhart JK, Kimmel CB. mef2ca is required in cranial neural crest to effect Endothelin1 signaling in zebrafish. Dev. Biol. 2007; 308:144–157. [PubMed: 17574232]

Moore CA, Parkin CA, Bidet Y, Ingham PW. A role for the Myoblast city homologues Dock1 and Dock5 and the adaptor proteins Crk and Crk-like in zebrafish myoblast fusion. Development. 2007; 134:3145–3153. [PubMed: 17670792]

Neyt C, Jagla K, Thisse C, Thisse B, Haines L, Currie PD. Evolutionary origins of vertebrate appendicular muscle. Nature. 2000; 408:82–86. [PubMed: 11081511]

Nowlan NC, Bourdon C, Dumas G, Tajbakhsh S, Prendergast PJ, Murphy P. Developing bones are differentially affected by compromised skeletal muscle formation. Bone. 2010; 46:1275–1285. [PubMed: 19948261]

Oates AC, Pratt SJ, Vail B, Yan Y, Ho RK, Johnson SL, Postlethwait JH, Zon LI. The zebrafish klf gene family. Blood. 2001; 98:1792–1801. [PubMed: 11535513]

Patapoutian A, Yoon JK, Miner JH, Wang S, Stark K, Wold B. Disruption of the mouse MRF4 gene identifies multiple waves of myogenesis in the myotome. Development. 1995; 121:3347–3358. [PubMed: 7588068]

Piotrowski T, Nüsslein-Volhard C. The endoderm plays an important role in patterning the segmented pharyngeal region in zebrafish (Danio rerio). Dev. Biol. 2000; 225:339–356. [PubMed: 10985854]

Rao PK, Kumar RM, Farkhondeh M, Baskerville S, Lodish HF. Myogenic factors that regulate expression of muscle-specific microRNAs. Proc. Natl. Acad. Sci. USA. 2006; 103:8721–8726. [PubMed: 16731620]

Rawls A, Valdez MR, Zhang W, Richardson J, Klein WH, Olson EN. Overlapping functions of the myogenic bHLH genes MRF4 and MyoD revealed in double mutant mice. Development. 1998; 125:2349–2358. [PubMed: 9609818]

Robling AG. Is bone's response to mechanical signals dominated by muscle forces? Med. Sci. Sports Exerc. 2009; 41:2044–2049. [PubMed: 19812512]

Rudnicki MA, Braun T, Hinuma S, Jaenisch R. Inactivation of MyoD in mice leads to up-regulation of the myogenic HLH gene Myf-5 and results in apparently normal muscle development. Cell. 1992; 71:383–390. [PubMed: 1330322]

Sambasivan R, Gayraud-Morel B, Dumas G, Cimper C, Paisant S, Kelly RG, Tajbakhsh S. Distinct regulatory cascades govern extraocular and pharyngeal arch muscle progenitor cell fates. Dev. Cell. 2009; 16:810–821. [PubMed: 19531352]

Sambasivan R, Kuratani S, Tajbakhsh S. An eye on the head: the development and evolution of craniofacial muscles. Development. 2011; 138:2401–2415. [PubMed: 21610022]

Schwarz JJ, Chakraborty T, Martin J, Zhou J, Olson EN. The basic region of myogenin cooperates with two transcription activation domains to induce muscle-specific transcription. Mol. Cell. Biol. 1992; 12:266–275. [PubMed: 1309591]

Sweetman D, Goljanek K, Rathjen T, Oustanina S, Braun T, Dalmay T, Munsterberg A. Specific requirements of MRFs for the expression of muscle specific microRNAs, miR-1, miR-206 and miR-133. Dev. Biol. 2008; 321:491–499. [PubMed: 18619954]

Theis S, Patel K, Valasek P, Otto A, Pu Q, Harel I, Tzahor E, Tajbakhsh S, Christ B, Huang R. The occipital lateral plate mesoderm is a novel source for vertebrate neck musculature. Development. 2011; 137:2961–2971. [PubMed: 20699298]

Tiidus PM, Bombardier E, Xeni J, Bestic NM, Vandenboom R, Rudnicki MA, Houston ME. Elevated catalase activity in red and white muscles of MyoD gene-inactivated mice. Biochem. Mol. Biol. Int. 1996; 39:1029–1035. [PubMed: 8866021]

Valdez MR, Richardson JA, Klein WH, Olson EN. Failure of Myf5 to support myogenic differentiation without myogenin, MyoD, and MRF4. Dev. Biol. 2000; 219:287–298. [PubMed: 10694423]

Venuti JM, Morris JH, Vivian JL, Olson EN, Klein WH. Myogenin is required for late but not early aspects of myogenesis during mouse development. J. Cell Biol. 1995; 128:563–576. [PubMed: 7532173]

Verzi MP, Agarwal P, Brown C, McCulley DJ, Schwarz JJ, Black BL. The Transcription Factor MEF2C Is Required for Craniofacial Development. Dev. Cell. 2007; 12:645–652. [PubMed: 17420000]

Vinagre T, Moncaut N, Carapuco M, Novoa A, Bom J, Mallo M. Evidence for a myotomal Hox/Myf cascade governing nonautonomous control of rib specification within global vertebral domains. Dev. Cell. 2010; 18:655–661. [PubMed: 20412779]

Vivian JL, Olson EN, Klein WH. Thoracic skeletal defects in myogenin- and MRF4-deficient mice correlate with early defects in myotome and intercostal musculature. Dev. Biol. 2000; 224:29–41. [PubMed: 10898959]

Walker MB, Kimmel CB. A two-color acid-free cartilage and bone stain for zebrafish larvae. Biotech. Histochem. 2007; 82:23–28. [PubMed: 17510811]

Wang ZZ, Washabaugh CH, Yao Y, Wang JM, Zhang L, Ontell MP, Watkins SC, Rudnicki MA, Ontell M. Aberrant development of motor axons and neuromuscular synapses in MyoD-null mice. J. Neurosci. 2003; 23:5161–5169. [PubMed: 12832540]

Weinberg ES, Allende ML, Kelly CS, Abdelhamid A, Murakami T, Andermann P, Doerre OG, Grunwald DJ, Riggleman B. Developmental regulation of zebrafish MyoD in wild-type, no tail and spadetail embryos. Development. 1996; 122:271–280. [PubMed: 8565839]

Westerfield, M. The Zebrafish Book - a guide for the laboratory use of zebrafish (Danio rerio). 3 ed. University of Oregon Press; 1995.

Williams AH, Valdez G, Moresi V, Qi X, McAnally J, Elliott JL, Bassel-Duby R, Sanes JR, Olson EN. MicroRNA-206 delays ALS progression and promotes regeneration of neuromuscular synapses in mice. Science. 2009; 326:1549–1554. [PubMed: 20007902]

Xu Y, He J, Wang X, Lim TM, Gong Z. Asynchronous activation of 10 muscle-specific protein (MSP) genes during zebrafish somitogenesis. Dev. Dyn. 2000; 219:201–215. [PubMed: 11002340]

Yablonka-Reuveni Z, Rudnicki MA, Rivera AJ, Primig M, Anderson JE, Natanson P. The transition from proliferation to differentiation is delayed in satellite cells from mice lacking MyoD. Dev. Biol. 1999; 210:440–455. [PubMed: 10357902]

Zhang W, Behringer RR, Olson EN. Inactivation of the myogenic bHLH gene MRF4 results in up-regulation of myogenin and rib anomalies. Genes Dev. 1995; 9:1388–1399. [PubMed: 7797078]
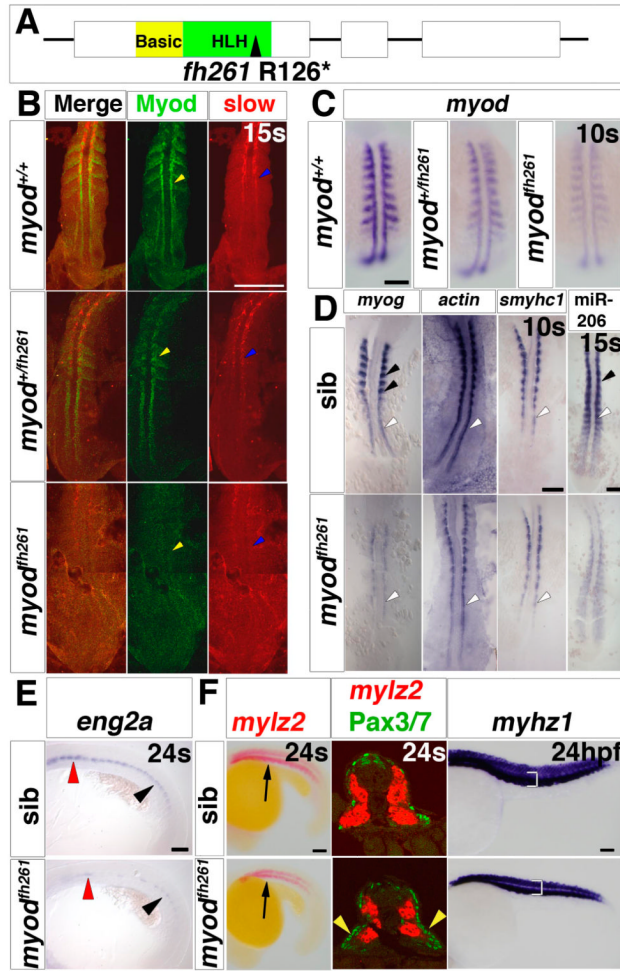
Fig. 1. *Myod*^{fh261} **mutants have delayed muscle differentiation**
A. Schematic of Myod gene and protein showing the *fh261* arginine to stop mutation within the helix-loop-helix domain, which is essential for dimerisation and DNA binding. **B.** Dual immunodetection of Myod and slow myosin in embryos from a *myod*$^{fh261/+}$ incross, genotyped by sequencing of genomic PCR. Dorsal view, anterior to top. **C.** In situ mRNA hybridization reveals reduction in *myod* mRNA in embryos from a *myod*$^{fh261/+}$ incross. Wholemount, anterior to top. **D-F.** In situ mRNA hybridization for indicated probes on *myod*^{fh261} mutants and their siblings. **D.** Adaxial slow precursors show reduced *myog* and *smyhc1* at 10s and miR-206 at 15s, but *actin* mRNA appeared less affected (white arrowheads). Fast muscle precursors had no *myog* or miR-206 expression at this stage (black arrowheads). Dorsal flatmount, anterior to top. **E.** *eng2a* expression is reduced in *myod*^{fh261} mutant in regions of muscle pioneers (black arrowhead) and medial fast fibres (red arrowhead). Lateral wholemount, anterior to left. **F.** Embryos labelled for fast *mylz2* with Fast Red were cryo-sectioned at the region indicated (arrow, left panels). Immunofluorescent detection of Pax3/7 protein revealed increased nuclei in the lateral somite in *myod*^{fh261} mutants (yellow arrowheads). Dorsoventral extent of fast *myhz1* mRNA (bracket, right panels) is reduced in *myod*^{fh261} mutants at 24 hpf. Lateral wholemounts, anterior to left. Bars = 100 μm.
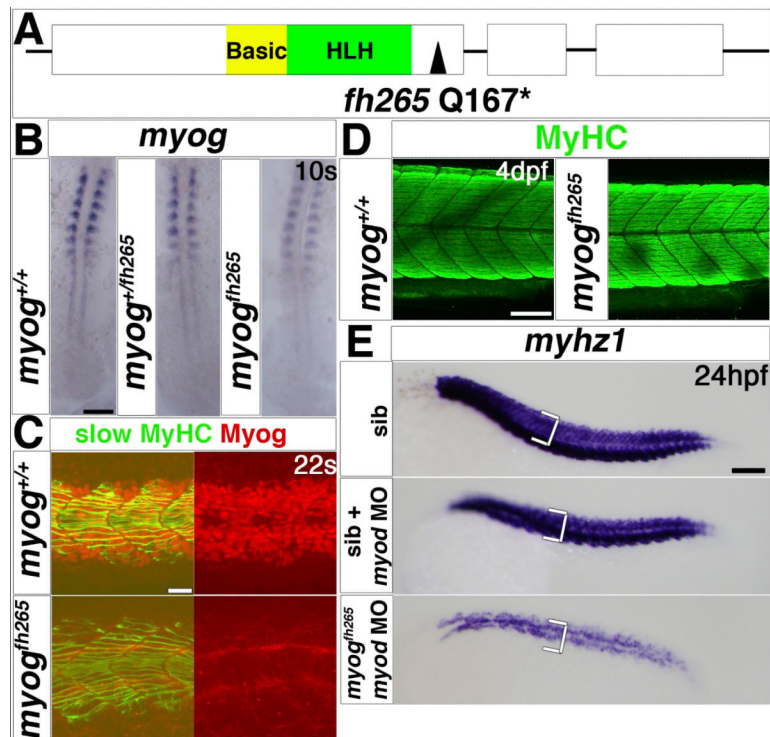
**Fig. 2. Myogenin cooperates with Myod in fast myogenesis**
A. Schematic of Myog gene and protein showing the *fh265* glutamine to stop mutation following the helix-loop-helix domain. **B-E.** *In situ* mRNA hybridization for *myog* (B) *or myhz1* (E) or immunodetection of Myog and slow MyHC (C) or MyHC (D) in *myog*$^{+/fh265}$ incrosses, injected with *myod* morpholino as indicated (E). **B.** Expression of *myog* mRNA is little affected in *myog*^{fh265} mutants. Dorsal flatmounts, anterior to top. **C.** Nuclear immunoreactivity with a polyclonal anti-rat Myog antibody is lost in *myog*^{fh265} mutants at 22s. **D.** All embryos from a *myog*$^{+/fh265}$ incross show normal levels of MyHC at 4 dpf. **E.** No change in *myhz1* mRNA is detected in *myog*^{fh265} mutants at 24 hpf (top panel). Injection of *myod* MO into *myog*^{fh265} (bottom panel) leads to a greater loss of fast muscle than when injected into their siblings (middle panel), which are comparable to *myod*^{fh261} mutants (see Fig. 1F). Lateral views, anterior to left (C-E). Bars = 100 µm (except C = 20 µm).
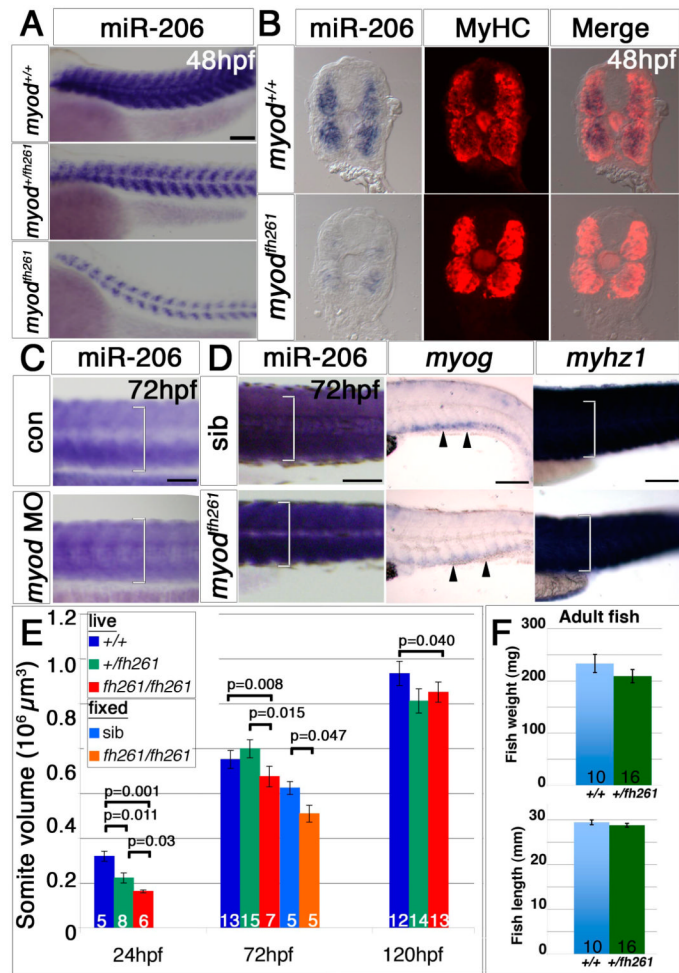
Fig. 3. Muscle growth is impaired in *myod^fh261* mutants

In situ mRNA hybridization for miR-206, *myog* and *myhz1* and immunodetection of MyHC. Lateral (A,C,D) views, anterior to left or transverse cryosections (B). **A.** miR-206 in sequence-genotyped 48 hpf embryos from a *myod^+/fh261* incross is primarily in fast fibres and is strongly reduced. **B.** Embryos from A were sectioned and stained with MyHC. miR-206 expression is strongly reduced in *myod^fh261* mutants compared with their siblings, while MyHC immunodetection is only mildly reduced. **C.** At 72hpf, miR-206 has increased in *myod* morphants, but is still less than in siblings. **D.** Compared to sibs, *myod^fh261* mutants (identified by head muscle defects) had less *myog* mRNA (arrowheads) and reduction in dorsoventral extent of somitic miR-206 and *myhz1* mRNA (brackets). **E.** Somite volume increases with age, but is reduced in *myod^fh261* mutant. These differences were consistent in live and fixed embryos. Number of embryos per condition are shown on columns and t-test statistics are indicated above columns. **F.** Adult fish mass and length. Bars = 100 μm.
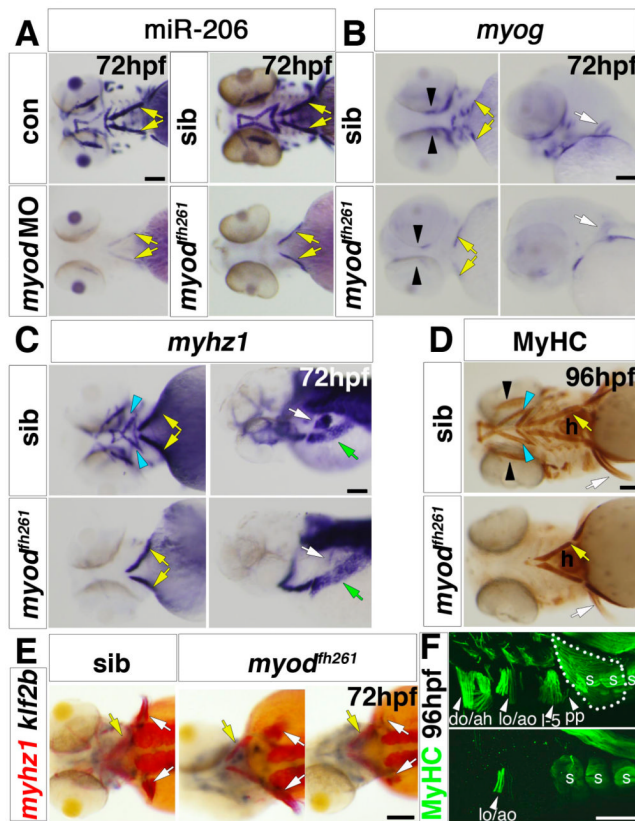
Fig. 4. *Myod^{fh261}* mutants lack head muscles and have defects in cartilage morphogenesis
In situ RNA hybridisation for miR-206 (A), *myog* (B), *myhz1* (C, E) and *klf2b* (E) or immunodetection of MyHC (MF20, D; A4.1025, F). Ventral (A, D and left panels of B and C), lateral (F, right panels of B and C) or dorsal (E) views, anterior to left. **A.** *Myod* morphant and *myod^{fh261}* mutant have similar loss of most cranial muscles except sternohyoideus (yellow arrows). **B-D.** In *myod^{fh261}* mutants, *myog* and *myhz1* mRNAs and MyHC are lost from many cranial muscles (blue arrows). Expression remains in sternohyoideus (yellow arrows), Weak *myog* mRNA is detected in adductor mandibulae (B, black arrows) and occasional fibres differentiate in adductor mandibulae. Hypaxial muscles (C, green arrows) seem unaffected and pectoral fin muscles (B-F, white arrows, dotted area in F) are variably reduced. **E.** In *myod^{fh261}* mutants, most head muscles are consistently missing, even though sternohyoid (yellow arrows) and cartilage precursors expressing *klf2b* are present, Pectoral fin muscle is variably reduced (white arrows). **F.** Higher magnification shows that levator and adductor operculi are partially spared in *myod^{fh261}* mutants, whereas pectoral fin and other muscles are missing, revealing the underlying somitic muscle (s). do dilatator operculi, ah adductor hyomandibulae, lo levator operculi, ao adductor operculi, l-5 levator 5, pp protractor pectoralis, Bars = 100 μm.
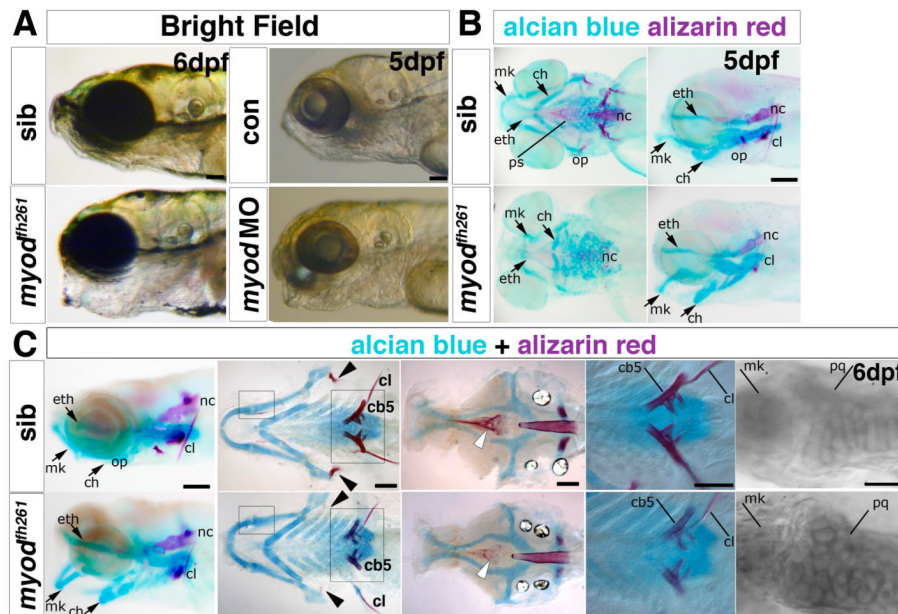
**Fig. 5.** *Myod^{fh261}* **mutants have cranial bone defects**

A. Bright field image of a live 6 dpf *myod^{fh261}* mutant (retrospectively sequence genotyped) and a 5 dpf *myod* morphant showing craniofacial defects of lowered jaw and open mouth compared with sibling and control, respectively. **B,C.** Alcian blue and alizarin red double staining for cartilage and bone in *myod^{fh261}* mutants and siblings. At 5 dpf (B), cartilage components in mutants have different morphology with the whole lower jaw dropping, forming a gaping mouth. Both first and second arch derivatives, such as Meckel's (mk) and ceratohyal (ch) cartilage respectively, are bent ventrally. The ethmoid plate (eth) is only mildly affected. Little bone staining is detected in the mutant. Anterior to left, ventral (left panel) and lateral (right panel) views. At 6 dpf (C), *myod^{fh261}* mutants show various cartilage and bone defects; the opercle (arrowheads) is missing, ceratobranchial 5 and the parasphenoid (white arrows) less ossified bone and the cleithrum is reduced. Cartilage cells in the mutant remain rounded, failing to mature into flattened columns. Anterior to left. Wholemounts in lateral view (left panel), or flatmounts of the dissected pharyngeal skeleton (ventral view, second from left) or neurocranium (dorsal view, central panel). Large boxed areas are magnified in the fourth panels, showing reduced ossification of ceratobranchial 5 and cleithrum. Small boxed areas are magnified in righthandmost panels to reveal rounded morphology of cartilage cells in the joint between Meckel's and palatoquadrate (pq) cartilages in the *myod^{fh261}* mutant. cl, cleithrum; nc, notochord; op, opercle; ps, parasphenoid; cb5 ceratobranchial 5. Bars = 100 µm.
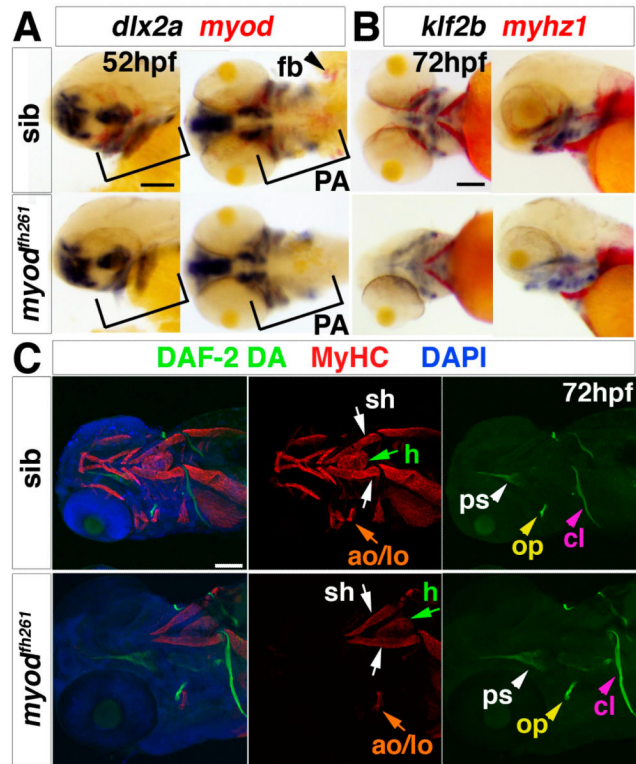
Fig. 6. Early cranial skeletal development is normal in m*yod^{fh261}* mutants

A,B. In situ mRNA hybridisation for *dlx2a* and *myod* (A), *klf2b* and *myhz1* (B) in 52 hpf (A) and 72 hpf (B) *myod^{fh261}* mutant and sibling embryos, shown in wholemount, anterior to left. Outer panels, lateral view, central panels, ventral view. *Myod* mRNA is absent but *dlx2a* unaffected in the pharyngeal arches (PA, brackets). *Myhz1* mRNA is detected in sternohyoideus (sh, arrows) but not in other head muscles in the mutant. *klf2b* mRNA in skeletal parts is normal. **C.** Confocal stacks of heads of *myod^{fh261}* mutant and sibling stained with DAF-2DA (green), MyHC (MF20, red) and DAPI (blue). Anterior to left, ventrolateral view. Muscle in the mutant is missing except for the sternohyoideus (sh, white arrows), adductor operculi and levator operculi (ao and lo, orange arrows). Bones such as the opercle (op, yellow arrowhead), cleithrum (cl, pink arrowheads) and parasphenoid (ps, white arrowheads) are normal at this stage. Bar = 100 μm.
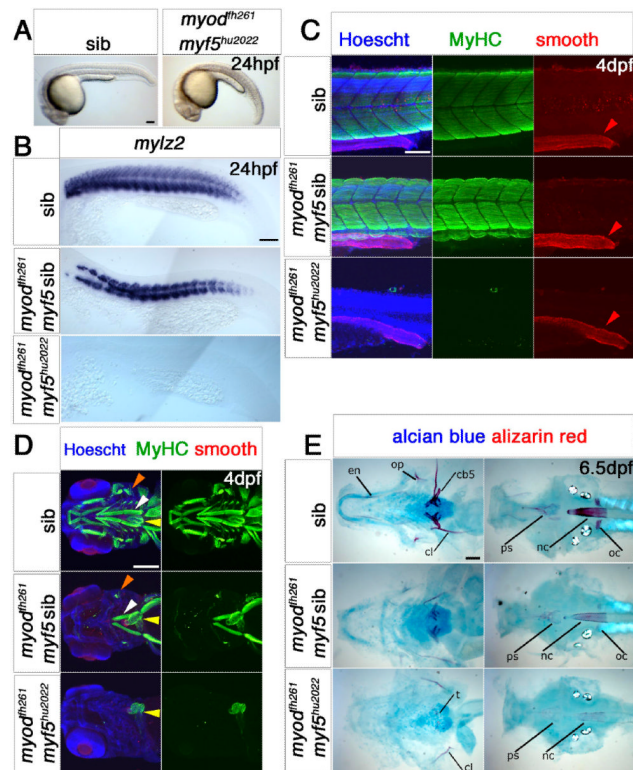
Fig. 7. Myf5 or Myod is required for myogenesis
Wholemounts (A), flatmounts (B) and confocal stacks (C,D) in lateral (A-C) or ventral (D) view of zebrafish embryos from $myf5^{hu2022/+}$;$myod^{fh261/+}$ in-cross analysed at the indicated stage by *in situ* mRNA hybridization for $mylz2$ (B) or immunohistochemistry for all-MyHC (green), smooth muscle myosin heavy chain 11 (red) and Hoechst (blue) in C,D, anterior to left. **A.** By 24 hpf, double mutant embryos are curved and have misshapen somites with signs of cell death. **B.** mRNA encoding fast myosin is reduced in putative $myod^{fh261}$ mutants and absent in doubles. **C.** Confocal stacks of somite-16 region at 4 dpf embryos show that no skeletal muscle *MyHC* is detected in genotyped double mutants, in which embryos are severely reduced in size. Smooth muscle myosin in the gut (red arrowheads) are unaffected. **D.** Confocal stacks of the head region of 4 dpf embryos show that all skeletal muscle is missing in $myf5^{hu2022}$;$myod^{fh261}$ double mutant, while heart (yellow arrows) and smooth muscle are intact. $myod^{fh261}$ mutant is missing all muscle except for the sternohyoideus (white arrows), adductor operculi and levator operculi (orange arrows). **E.** Alcian blue and alizarin red double staining for cartilage and bone in 6.5 dpf $myf5^{hu2022}$;$myod^{fh26\ 1}$ shows a more severe phenotype than in $myod^{fh261}$ mutants and siblings. Flatmounts of the dissected pharyngeal skeleton (ventral view, left panels) or neurocranium (dorsal view, right panels). Cartilage components in double mutants stain poorly. Bone is only detected in the double mutant in cleithrum (cl) and teeth (left panel) and faintly in the notochord (nc) and parasphenoid (ps) (right panel). oc, occipitals; op, opercle; en, enteropterygoid; cb5, ceratobranchial 5. Bars = 100 μm.